

# Oxidase activity of a flavin-dependent thymidylate synthase

Zhen Wang<sup>1</sup>, Anatoly Chernyshev<sup>1</sup>, Eric M. Koehn<sup>1</sup>, Tony D. Manuel<sup>1</sup>, Scott A. Lesley<sup>2</sup> and Amnon Kohen<sup>1</sup>

<sup>1</sup> Department of Chemistry, University of Iowa, Iowa City, IA, USA

<sup>2</sup> The Joint Center for Structural Genomics at The Genomics Institute of Novartis Research Foundation, San Diego, CA, USA

## Keywords

competitive substrates; enzyme kinetics; flavin; oxidase; thymidylate synthase

## Correspondence

A. Kohen, Department of Chemistry, University of Iowa, Iowa City, IA 52242, USA

Fax: +1 319 335 1270

Tel: +1 319 335 0234

E-mail: amnon-kohen@uiowa.edu

Website: <http://cricket.chem.uiowa.edu/~kohen/>

(Received 3 February 2009, revised 10 March 2009, accepted 12 March 2009)

doi:10.1111/j.1742-4658.2009.07003.x

Flavin-dependent thymidylate synthases (FDTS) catalyze the production of dTMP from dUMP and N<sup>5</sup>,N<sup>10</sup>-methylene-5,6,7,8-tetrahydrofolate (CH<sub>2</sub>H<sub>4</sub>folate). In contrast to human and other classical thymidylate synthases, the activity of FDTS depends on a FAD coenzyme, and its catalytic mechanism is very different. Several human pathogens rely on this recently discovered enzyme, making it an attractive target for novel antibiotics. Like many other flavoenzymes, FDTS can function as an oxidase, which catalyzes the reduction of O<sub>2</sub> to H<sub>2</sub>O<sub>2</sub>, using reduced NADPH or other reducing agents. In this study, we exploit the oxidase activity of FDTS from *Thermatoga maritima* to probe the binding and release features of the substrates and products during its synthase activity. Results from steady-state and single-turnover experiments suggest a sequential kinetic mechanism of substrate binding during FDTS oxidase activity. CH<sub>2</sub>H<sub>4</sub>folate competitively inhibits the oxidase activity, which indicates that CH<sub>2</sub>H<sub>4</sub>folate and O<sub>2</sub> compete for the same reduced and dUMP-activated enzymatic complex (FDTS-FADH<sub>2</sub>-NADP<sup>+</sup>-dUMP). These studies imply that the binding of CH<sub>2</sub>H<sub>4</sub>folate precedes NADP<sup>+</sup> release during FDTS activity. The inhibition constant of CH<sub>2</sub>H<sub>4</sub>folate towards the oxidase activity was determined to be rather small (2 μM), which indicates a tight binding of CH<sub>2</sub>H<sub>4</sub>folate to the FDTS-FADH<sub>2</sub>-NADP<sup>+</sup>-dUMP complex.

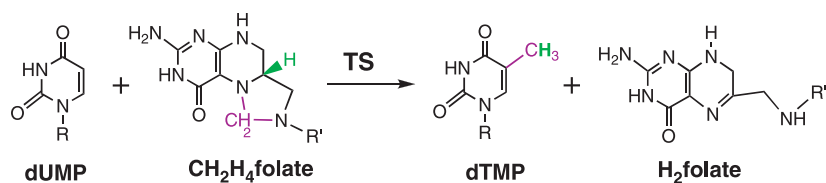
Thymidylate synthases [TS, encoded by the *thyA* and *tymS* genes – the gene that codes for TS (EC 2.1.1.45) in mouse, rat and human is currently named *tymS* rather than *thyA*] catalyze the reductive methylation of dUMP to form dTMP in nearly all eukaryotes, including humans. This reaction employs N<sup>5</sup>,N<sup>10</sup>-methylene-5,6,7,8-tetrahydrofolate (CH<sub>2</sub>H<sub>4</sub>folate) as both the methylene and the hydride donor [1], producing 7,8-dihydrofolate (H<sub>2</sub>folate), as illustrated in Scheme 1. The product, H<sub>2</sub>folate, is reduced to 5,6,7,8-tetrahydrofolate (H<sub>4</sub>folate) by dihydrofolate reductase (encoded by the *folA* gene), and then methylenated back to CH<sub>2</sub>H<sub>4</sub>folate.

The genomes of *thyA*-dependent organisms have been found to contain *folA* as well, forming a TS-dihydrofolate reductase-coupled catalytic cycle that is essential for thymidine biosynthesis.

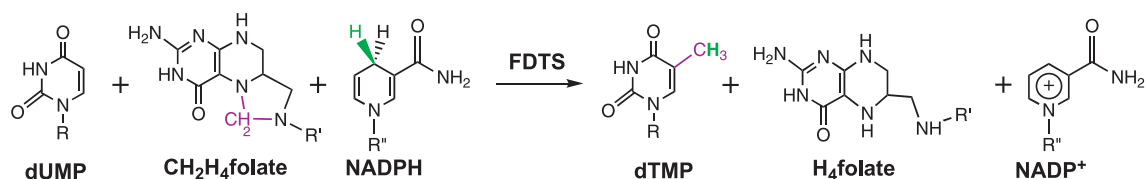
Since 2002, *thyX*, a new gene that codes for flavin-dependent thymidylate synthases (FDTS), has been identified in a number of microorganisms, including some severe human pathogens [2–5]. FDTS is a homotetramer with four identical active sites, each of which is formed at an interface of three of the four subunits [6]. This is quite different from the structure of classical TS, which is a homodimer with one active

## Abbreviations

CH<sub>2</sub>H<sub>4</sub>folate, N<sup>5</sup>,N<sup>10</sup>-methylene-5,6,7,8-tetrahydrofolate; FDTS, flavin-dependent thymidylate synthase; H<sub>2</sub>folate, 7,8-dihydrofolate; H<sub>4</sub>folate, 5,6,7,8-tetrahydrofolate; TS, thymidylate synthase.



**Scheme 1.** The reaction catalyzed by classical TS. **R** is 2'-deoxyribose-5'-phosphate and **R'** is *p*-aminobenzoyl-glutamate.



**Scheme 2.** The reaction catalyzed by FDTS. **R** is 2'-deoxyribose-5'-phosphate, **R'** is *p*-aminobenzoyl-glutamate and **R''** is adenine-2'-phosphate-ribose-5'-pyrophosphate-ribose.

site per subunit [1]. Recent studies have suggested that the catalytic mechanisms of TS and FDTS also differ substantially [7–10]. Because dTMP is a vital metabolite for DNA biosynthesis, this newly discovered enzyme is a promising target for novel antibiotics that could be designed to selectively inhibit FDTS activity and show potentially low toxicity for humans.

In order to direct future drug design, the molecular mechanism by which FDTS catalyzes thymidylate synthesis must be clarified to reveal the enzyme–substrate complexes and intermediates present along the reaction pathway. In contrast to classical TS, FDTS takes the hydride from reduced nicotinamides or other reductants, whereas CH<sub>2</sub>H<sub>4</sub>folate serves as the methylene donor only and produces H<sub>4</sub>folate instead of H<sub>2</sub>folate (Scheme 2) [2,4,5]. This difference explains the absence of both *thyA* and *folA* in the genomes of some *thyX*-dependent organisms [11]. Preliminary studies have shown that the FDTS mechanism is substantially different from the common bifunctional enzymes with both TS and dihydrofolate reductase activities [7–9]. During the reductive half-reaction, NADPH reduces the noncovalently bound FAD cofactor to FADH<sub>2</sub>; during the oxidative half-reaction, the enzyme catalyzes transfer of the methylene group from CH<sub>2</sub>H<sub>4</sub>folate to dUMP, and FADH<sub>2</sub> serves as the reducing agent to produce dTMP. Several proposed kinetic mechanisms suggested that the product of the reductive half-reaction (NADP<sup>+</sup>) leaves before CH<sub>2</sub>H<sub>4</sub>folate binds to the enzyme [7–9]. This putative kinetic mechanism, however, remains to be experimentally tested.

Like many other flavoenzymes, FDTS can function as an NADPH oxidase, consuming molecular O<sub>2</sub> and

producing NADP<sup>+</sup> and H<sub>2</sub>O<sub>2</sub>. Our recent studies revealed a close connection between the synthase activity (dUMP → dTMP) and oxidase activity (O<sub>2</sub> → H<sub>2</sub>O<sub>2</sub>) of FDTS [12,13]. To date, however, several aspects of the proposed mechanism have not been confirmed experimentally. Here, we report pre-steady-state and steady-state studies on the oxidase activity of FDTS from *Thermotoga maritima*, and elucidate the binding and release features of its synthase substrates NADPH, CH<sub>2</sub>H<sub>4</sub>folate and dUMP.

## Results and Discussion

### Initial velocity studies of FDTS oxidase activity

Previous studies suggested that NADPH binds to the FDTS–FAD complex, and that after flavin is reduced, the product of the reductive half-reaction, NADP<sup>+</sup>, dissociates before initiation of the oxidative half-reaction [7–9]. This proposed mechanism was examined by measuring the steady-state initial velocities of FDTS oxidase activity while varying NADPH at several O<sub>2</sub> concentrations (8, 20, 50 and 210 μM, 1 mM). These experiments were conducted in the presence of saturating concentrations of dUMP, to ensure examination of the dUMP-activated form of the enzyme [12,13]. The results revealed that, in the absence of CH<sub>2</sub>H<sub>4</sub>folate, FDTS oxidase activity exhibits Michaelis–Menten kinetics for O<sub>2</sub> with an unusually small *K<sub>m</sub>* value. The apparent *K<sub>m</sub>* values of O<sub>2</sub> at 100 μM NADPH were 7 ± 1 μM at 37 °C and 29 ± 2 μM at 65 °C. This may imply that either the enzyme has a binding site for O<sub>2</sub> or, more likely, that

an O<sub>2</sub>-independent step becomes rate limiting as the concentration of O<sub>2</sub> increases [14].

The double-reciprocal Lineweaver–Burk plot (1/rate versus 1/[substrate]) of FDTS oxidase activity shows an intersecting pattern (Fig. 1), which suggests a sequential kinetic mechanism. If the product NADP<sup>+</sup> leaves the enzymatic complex before O<sub>2</sub> binds, these lines would be parallel (i.e. a ping-pong mechanism) [15,16]. The data were globally fit to a bi-substrate sequential mechanism (Eqn 1) [16] to estimate the kinetic parameters:

$$\frac{v}{[E]_t} = \frac{k_{\text{cat}}[A][B]}{K_{ia}K_b + K_a[B] + K_b[A] + [A][B]} \quad (1)$$

where [A], [B] and [E]<sub>t</sub> are the concentrations of NADPH and O<sub>2</sub>, and total concentration of enzyme active sites, respectively;  $K_a$  is the Michaelis–Menten constant of NADPH,  $K_b$  is the Michaelis–Menten constant of O<sub>2</sub>, and  $K_{ia}$  is the dissociation constant of the substrate from the enzymatic complex. The kinetic parameters determined from this global fitting are:  $k_{\text{cat}} = 0.0830 \pm 0.0002 \text{ s}^{-1}$ ,  $K_a = 522 \pm 2 \text{ }\mu\text{M}$ ,  $K_{ia} = 3.61 \pm 0.06 \text{ mM}$ ,  $K_b = 1.12 \pm 0.02 \text{ }\mu\text{M}$ .

#### Assessment of the rate of product NADP<sup>+</sup> release by examination of the FADH<sub>2</sub>–NADP<sup>+</sup> charge-transfer complex

The progress of the reductive half-reaction was monitored by recording UV–Vis spectra continuously in

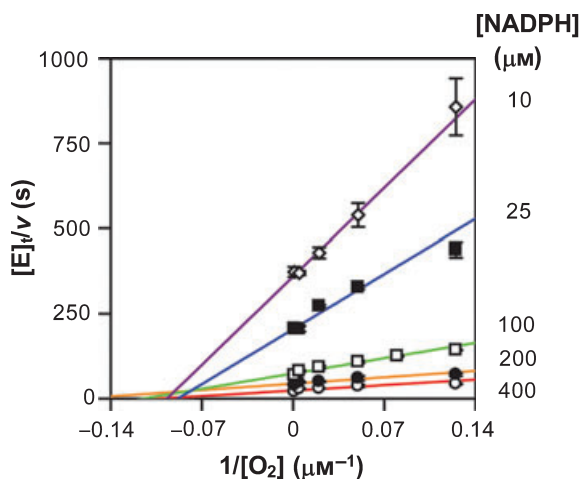


**Fig. 1.** Steady-state sequential mechanism of FDTS oxidase activity. Data are presented as a Lineweaver–Burk double-reciprocal plot. Experiments were performed at 37 °C. NADPH concentrations used were (○, red line) 400 μM, (●, orange line) 200 μM, (□, green line) 100 μM, (■, blue line) 25 μM and (◇, purple line) 10 μM.

anaerobic single-turnover experiments. The decrease in absorbance at 450 nm follows the reduction of enzyme-bound FAD. When NADPH is used as the reducing agent, the spectra also show an increase in the absorbance of a wide band (550–900 nm) with an isosbestic point at 510 nm (Fig. 2A). This wide band is not observed during FAD reduction by dithionite, and is identified as a charge-transfer complex between the reduced flavin and the oxidized nicotinamide [17–19]. The first-order rate constant of the formation of the charge-transfer complex was found to be identical to that of FAD reduction (Fig. 2A), which, together with the isosbestic point, indicates that the two changes occur simultaneously and represent the same process. This observation demonstrates the stability of the enzyme-bound FADH<sub>2</sub>–NADP<sup>+</sup> complex formed during the reductive half-reaction, and suggests the close proximity of the oxidized nicotinamide ring to the reduced isoalloxazine ring. This observation is significant because no other structural information is currently available regarding the binding site of the nicotinamide cofactor.

After completion of the reductive single-turnover experiment, the rate of NADP<sup>+</sup> release from the FDTS–FADH<sub>2</sub>–NADP<sup>+</sup>–dUMP complex was measured by following the disappearance of the charge-transfer band, while no change was observed at 450 nm (Fig. 2B). The rate constant of NADP<sup>+</sup> release was determined to be  $0.00135 \pm 0.00005 \text{ s}^{-1}$  at 37 °C (Fig. 2B). By comparison, the first-order rate constant of FADH<sub>2</sub> oxidation by O<sub>2</sub> was determined to be  $0.131 \pm 0.010 \text{ s}^{-1}$  at 0 °C in the oxidative single-turnover experiment. Thus, NADP<sup>+</sup> release from the enzyme is at least two orders of magnitude slower than FADH<sub>2</sub> oxidation by O<sub>2</sub>, indicating that NADP<sup>+</sup> has a very high affinity for the reduced enzyme. This suggests that NADP<sup>+</sup> does not leave the FDTS–FADH<sub>2</sub>–NADP<sup>+</sup>–dUMP complex at the end of the reductive half-reaction, but remains bound to the enzymatic complex during the oxidative half-reaction. This observation supports the sequential mechanism suggested above from steady-state kinetic measurements. Neither the rate of FAD reduction nor that of FADH<sub>2</sub>–NADP<sup>+</sup> formation is dependent on dUMP concentration, which confirms our previous suggestion that dUMP does not influence the reductive half-reaction [13].

#### Assessment of NADP<sup>+</sup> binding to the oxidized enzyme from product inhibition studies

Because NADP<sup>+</sup> appears to bind tightly to the reduced enzyme, it is of interest to assess its binding to

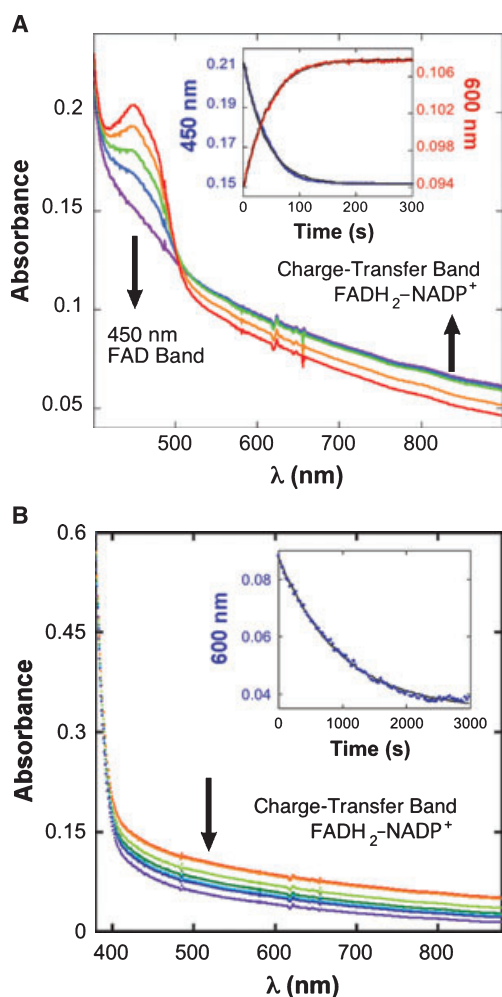


**Fig. 2.** The kinetics of  $\text{FADH}_2\text{-NADP}^+$  charge-transfer complex during the reductive half-reaction of FDTS. (A) Spectra of  $10\ \mu\text{M}$  (active-site concentration)  $tm\text{FDTS-FAD}$  being reduced anaerobically by  $200\ \mu\text{M}$  NADPH in  $200\ \text{mM}$  Tris/HCl buffer (pH 7.9) at  $37\ ^\circ\text{C}$ . Each spectrum was sampled at a different time during one single-turnover experiment. The absorbance of FAD (450 nm) decreases as the charge-transfer band of the  $\text{FADH}_2\text{-NADP}^+$  complex (550–900 nm) increases. (Inset) A typical time course of the enzyme-bound FAD reduction by NADPH. The decrease of absorbance at 450 nm is presented as red traces, and the increase of the charge-transfer band from 550 to 900 nm is presented as blue traces. Fitting each time course (black curves in the inset) to an exponential equation yields a first-order rate constant, both equal  $0.025 \pm 0.002\ \text{s}^{-1}$ . (B) Continuation of the experiments described in (A), but the first spectrum was recorded after the last one in (A), and the spectra were recorded in intervals of 30 min. The wide charge-transfer band disappears slowly while the enzyme remains reduced and with no change in total enzyme concentration (as judged from absorbance at 230–300 nm). The decrease in charge transfer band is interpreted as  $\text{NADP}^+$  release. The inset presents the exponential fitting (black curve) of the time course of absorbance change at 600 nm (blue traces). The first-order rate constant of disappearance of the charge-transfer band was determined to be  $0.00135 \pm 0.00005\ \text{s}^{-1}$ .

the oxidized enzyme. In addition, product inhibition studies can discriminate between the steady-state ordered and random mechanisms, which is not easy to do via initial velocity measurements in the absence of products [15,16]. Therefore, the effect of  $\text{NADP}^+$  on initial velocities was examined by measuring the steady-state initial velocities of FDTS oxidase activity with  $100\ \mu\text{M}$  NADPH at both saturating ( $210\ \mu\text{M}$ ) and sub-saturating ( $10\ \mu\text{M}$ )  $\text{O}_2$  concentrations. These measurements show no observable inhibition up to the solubility limit of  $\sim 550\ \text{mM}$   $\text{NADP}^+$  under the experiment conditions. Regardless of the enzymatic complex from which  $\text{NADP}^+$  dissociates, the lack of any inhibitory effect corroborates the low affinity of  $\text{NADP}^+$  for the oxidized enzyme, despite its high affinity for the reduced enzyme.

### Inhibition of FDTS oxidase activity by $\text{CH}_2\text{H}_4\text{folate}$

$\text{CH}_2\text{H}_4\text{folate}$  appears to inhibit FDTS oxidase activity, and the addition of  $400\ \mu\text{M}$   $\text{CH}_2\text{H}_4\text{folate}$  completely suppresses this activity under atmospheric  $\text{O}_2$  concentrations ( $210\ \mu\text{M}$ ). In order to investigate the nature of inhibition of FDTS oxidase activity by  $\text{CH}_2\text{H}_4\text{folate}$ , steady-state initial velocities were measured while varying  $\text{CH}_2\text{H}_4\text{folate}$  concentrations at several  $\text{O}_2$  concentrations (8, 12.5, 20 and  $210\ \mu\text{M}$ , 1 mM), in the presence of a saturating concentration of dUMP. The initial velocities under an atmospheric  $\text{O}_2$  concentration were also studied in the absence of dUMP, and although the rates are slower [13], dUMP does not seem to affect the nature of  $\text{CH}_2\text{H}_4\text{folate}$  inhibition of the oxidase activity. To examine the relation between  $\text{CH}_2\text{H}_4\text{folate}$  and  $\text{O}_2$ , and to ascertain the binding constant of  $\text{CH}_2\text{H}_4\text{folate}$  to the reduced and dUMP-activated enzyme, we used a simplified model in which  $\text{CH}_2\text{H}_4\text{folate}$  is treated as a dead-end inhibitor [15,16] of the oxidase activity. The validity of this simplification is examined and verified in the Appendix.

To determine the inhibition pattern of  $\text{CH}_2\text{H}_4\text{folate}$  toward  $\text{O}_2$ , initial velocities were analyzed by the secondary slope and intercept replots of the Lineweaver–Burk double-reciprocal plot (Fig. 3A) [16]. The slope of the double-reciprocal plot increases linearly with the concentration of  $\text{CH}_2\text{H}_4\text{folate}$  (Fig. 3B), although the intercept is independent of the concentration of  $\text{CH}_2\text{H}_4\text{folate}$  (Fig. 3C). According to this analysis,  $\text{CH}_2\text{H}_4\text{folate}$  appears to be a competitive inhibitor of  $\text{O}_2$  in FDTS oxidase activity. The initial velocities were thus fit to the competitive inhibition model to estimate the kinetic parameters [15,16]:

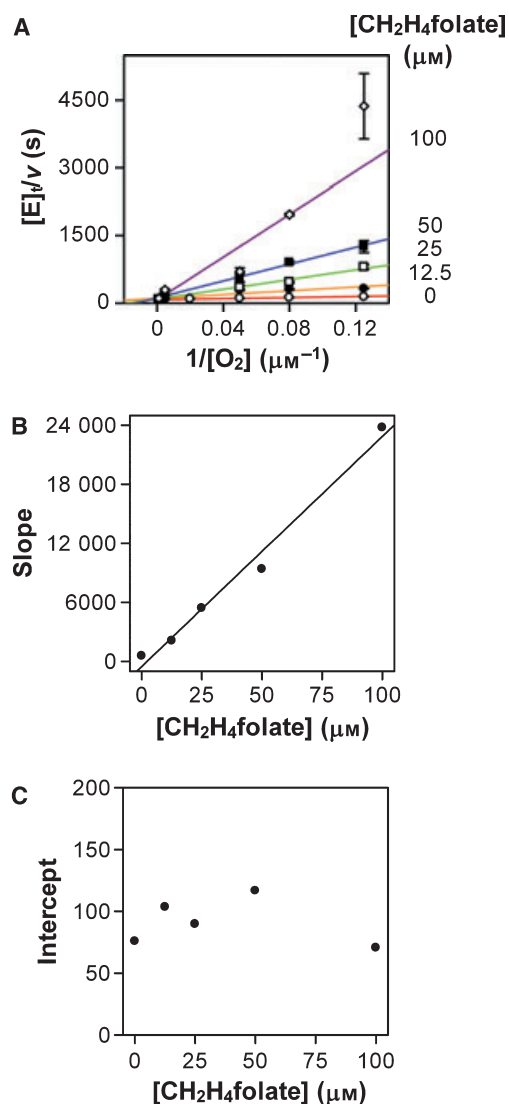


**Fig. 3.** Competitive inhibition of FDTS oxidase activity by CH<sub>2</sub>H<sub>4</sub>folate. (A) The Lineweaver–Burk double-reciprocal plot (1/rate versus 1/[O<sub>2</sub>]). CH<sub>2</sub>H<sub>4</sub>folate concentrations used were (○, red line) 0 μM, (●, orange line) 12.5 μM, (□, green line) 25 μM, (■, blue line) 50 μM and (◇, purple line) 100 μM. (B) Secondary slope-replot of the Lineweaver–Burk plot (A), which increases linearly with [CH<sub>2</sub>H<sub>4</sub>folate]. (C) Secondary intercept-replot of the Lineweaver–Burk plot (A), which is independent of [CH<sub>2</sub>H<sub>4</sub>folate]. Experiments were performed at 37 °C.

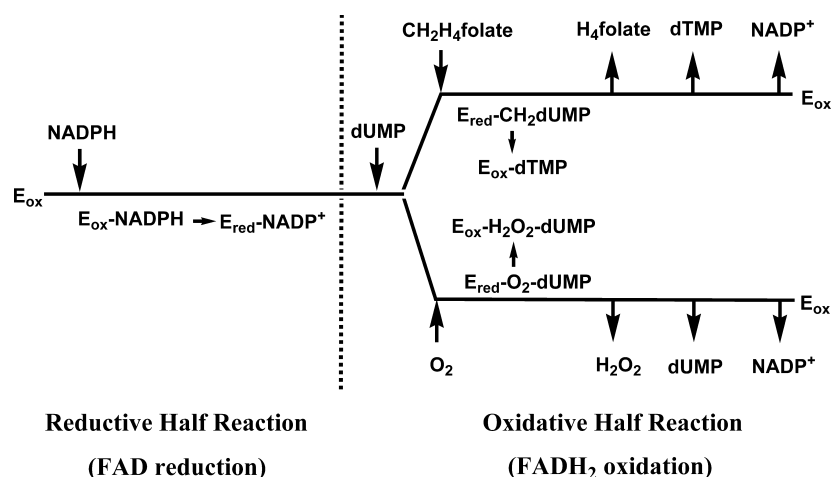
$$\frac{v}{[E]_t} = \frac{k_{\text{cat}}[S]}{K_m \left(1 + \frac{[I]}{K_I}\right) + [S]} \quad (2)$$

where  $k_{\text{cat}}$  is the first-order rate constant, describing the maximal reaction rate per enzyme active site; [S], [I] and  $[E]_t$  are the concentrations of O<sub>2</sub>, CH<sub>2</sub>H<sub>4</sub>folate

and total concentration of enzyme active sites, respectively;  $K_m$  is the Michaelis–Menten constant of O<sub>2</sub>, and  $K_I$  is the inhibition constant of CH<sub>2</sub>H<sub>4</sub>folate. The kinetic parameters determined from this fitting were:  $k_{\text{cat}} = 0.0127 \pm 0.0004 \text{ s}^{-1}$ ,  $K_m = 7 \pm 1 \text{ μM}$ ,  $K_I = 1.9 \pm 0.3 \text{ μM}$ . The inhibition pattern was also analyzed by globally fitting the initial velocities to the mixed-type inhibition model [15], which is a general equation for competitive, noncompetitive or uncompetitive inhibition. The results also suggest that the inhibition is best described by the competitive pattern. A detailed analysis is presented in the Appendix. In summary, the observed competitive inhibition of CH<sub>2</sub>H<sub>4</sub>folate towards O<sub>2</sub> indicates that CH<sub>2</sub>H<sub>4</sub>folate and O<sub>2</sub> compete for the same enzymatic complex (FDTS–FADH<sub>2</sub>–NADP<sup>+</sup>–dUMP).

The sequential binding order of NADPH and O<sub>2</sub> in FDTS oxidase activity, together with the competitive inhibition pattern between O<sub>2</sub> and CH<sub>2</sub>H<sub>4</sub>folate, suggests that the binding order of NADPH and CH<sub>2</sub>H<sub>4</sub>folate in FDTS synthase activity is also sequential. This conclusion disagrees with the kinetic schemes proposed in previous studies, in which NADP<sup>+</sup> leaves before the oxidation of FADH<sub>2</sub> [7–9]. A recent kinetic study on the synthase activity of FDTS from *Mycobacterium tuberculosis* corroborates our data [20]. The presence of NADP<sup>+</sup> in complexes during the oxidative half-reaction is important in various attempts to mimic these complexes, which may assist in the design of inhibitors and drugs, as well as in the crystallization of the long-sought enzymatic complexes with nicotinamide cofactors and/or folate derivatives.

The inhibition constant ( $K_I = 1.9 \pm 0.3 \text{ μM}$ ) obtained from this experiment is a direct measure of the dissociation constant of CH<sub>2</sub>H<sub>4</sub>folate from the FDTS–FADH<sub>2</sub>–NADP<sup>+</sup>–dUMP–CH<sub>2</sub>H<sub>4</sub>folate complex. This measurement affords a good estimate of the binding constant of CH<sub>2</sub>H<sub>4</sub>folate to the FDTS–FADH<sub>2</sub>–NADP<sup>+</sup>–dUMP complex ( $1/K_I \sim 0.5 \text{ μM}^{-1}$ ), which reflects the high affinity of CH<sub>2</sub>H<sub>4</sub>folate for the reduced and dUMP-activated enzyme. This complex seems to be unique to FDTS, therefore, such information may assist in the rational design of inhibitors and drugs. This is significant because, hitherto, no specific inhibitors or drugs targeting FDTS have been identified. The current finding may also direct efforts towards the crystallization of complexes of FDTS with FADH<sub>2</sub>, dUMP, NADP<sup>+</sup> and folate derivatives under anaerobic conditions. Solving structures with nicotinamide and folate entities would help identify the binding sites of both NADPH and CH<sub>2</sub>H<sub>4</sub>folate, and provide important structural information for FDTS studies.



**Scheme 3.** The proposed binding and release kinetic mechanism of FDTS (see text for details).  $E_{\text{red}}$  and  $E_{\text{ox}}$  represent the reduced and the oxidized enzymatic complexes, respectively. Adopted from Chernyshev *et al.* [13]. All the arrows represent reversible process but the formation of dTMP that appears to be irreversible.

### Kinetic scheme

Based on the results presented here and in previous studies [7–9,12,13], thymidylate synthesis catalyzed by FDTS follows a sequential kinetic mechanism with respect to all its substrates, as illustrated in Scheme 3. The reaction is composed of a reductive half-reaction and an oxidative half-reaction, and  $\text{NADP}^+$  only leaves the enzymatic complex after the oxidation of flavin. Because dUMP acts as an activator for the oxidative half-reaction, but not for the reductive half-reaction [12,13], we propose that it binds at the beginning of the oxidative half-reaction. After dUMP binds to and activates the enzyme,  $\text{CH}_2\text{H}_4\text{folate}$  and  $\text{O}_2$  compete for the reduced and dUMP-activated enzymatic complex. To date, no direct evidence has been shown to support the exact order of product release after the oxidation of  $\text{FADH}_2$ , so Scheme 3 follows a ‘first come, last leave’ principle.

### Conclusions

The oxidase activity of *Thermotoga maritima* FDTS was exploited to probe several aspects of the kinetic mechanism of FDTS-catalyzed thymidylate synthesis.  $\text{CH}_2\text{H}_4\text{folate}$  and  $\text{O}_2$  appear to be competitive substrates of FDTS, supporting the notion that both compete for the same reduced form of the enzyme (i.e. the FDTS- $\text{FADH}_2$ - $\text{NADP}^+$ -dUMP complex). The binding constant of  $\text{CH}_2\text{H}_4\text{folate}$  to the reduced form of the enzyme is determined to be rather large ( $1/K_1 = 0.5 \mu\text{M}$ ), suggesting a tightly bound reactive FDTS- $\text{FADH}_2$ - $\text{NADP}^+$ -dUMP- $\text{CH}_2\text{H}_4\text{folate}$  com-

plex. Binding constants of a substrate to a preactivated enzyme are usually difficult to measure. We developed a method to assess such a binding constant, by studying an alternative activity of the enzyme where the substrate of interest acts as an inhibitor (or competitive substrate, see Appendix). The high binding affinity of  $\text{CH}_2\text{H}_4\text{folate}$  to the reactive enzymatic complex, and the observation that the oxidase activity of FDTS is faster than the synthase activity, implies that steps following  $\text{CH}_2\text{H}_4\text{folate}$  binding are rate-limiting for the oxidative half-reaction of FDTS synthase activity. These results agree with previous observations that the presence of  $\text{CH}_2\text{H}_4\text{folate}$  slows the consumption of NADPH under aerobic conditions [8]. In addition, the oxidase activity of FDTS calls for caution when studying the synthase activity under aerobic conditions, which has been the case in many previous studies [2,5,8,9,20,21]. Aerobic experiments in which nonsaturating  $\text{CH}_2\text{H}_4\text{folate}$  concentrations were used may need to be revisited, whereas the results of kinetic measurements with saturating concentrations of  $\text{CH}_2\text{H}_4\text{folate}$  should be valid, as the oxidase activity of the FDTS would be completely suppressed.

In contrast to the suggestions from previous studies [7–9], our data indicate that the product of the reductive half-reaction,  $\text{NADP}^+$ , does not leave the enzymatic complex after the reductive half-reaction [20]. The findings identify a potentially stable complex of reduced FDTS with dUMP,  $\text{NADP}^+$  and folate derivatives (Scheme 3). The existence of such complexes may lead to new directions in inhibitor and drug design, as well as to direct attempts to gain structural information of FDTS complexes with folates and nicotinamides. The

lack of such information is currently a major obstacle to understanding FDTS in general.

## Materials and methods

All chemicals were purchased from Sigma-Aldrich (St. Louis, MO, USA), unless otherwise specified. Formaldehyde solution (37.3% by weight) was purchased from Fisher Scientific (Pittsburgh, PA, USA). CH<sub>2</sub>H<sub>4</sub>folate was a generous gift from Eprova Inc. (Schaffhausen, Switzerland). All chemicals were used as purchased without further purification. *Thermotoga maritima* FDTS (*tm*FDTS) enzyme was expressed and purified as previously described [6].

## Analytical methods

A Varian Cary 300 Bio UV–Vis spectrophotometer was used for concentration determinations and steady-state kinetic measurements. A Hewlett-Packard 8453 series diode-array UV–Vis spectrophotometer was used in single-turnover experiments. All the measured velocities were normalized by the concentration of enzyme active sites. All the reported concentrations refer to the final reaction mixture. FDTS concentration refers to its active-site concentration as determined from 450 nm absorbance of bound FAD ( $\epsilon_{450} = 11\,300\text{ M}^{-1}\text{cm}^{-1}$ ) [12]. To analyze the data from steady-state initial velocity measurements, kinetic parameters were assessed from least-square nonlinear regression of the data to the appropriate rate equation with GRAFIT 5.0. For graphical presentation and further analysis, we used the Lineweaver–Burk double-reciprocal plot and secondary replots to further discriminate the kinetic patterns [16].

## Steady-state kinetic measurements

Initial velocities of FDTS oxidase activity were measured with the coupled horseradish peroxidase (type VIA)/Amplex Red assay, by following the oxidation of Amplex Red by H<sub>2</sub>O<sub>2</sub> as indicated by the increase of absorbance at 575 nm ( $\epsilon_{575} = 67\,000\text{ M}^{-1}\text{cm}^{-1}$ ) [22]. Experiments were performed at 37 °C in 200 mM Tris/HCl buffer (pH 7.9), with 100  $\mu\text{M}$  dUMP (to ensure examination of the dUMP-activated enzyme) [13], 50  $\mu\text{M}$  Amplex Red, 1 unit·mL<sup>-1</sup> horseradish peroxidase and 2  $\mu\text{M}$  FDTS. Reactions were initiated by addition of FDTS. The final volume of the reaction mixture was 210  $\mu\text{L}$ . Three different Tris/HCl buffers were prepared: (a) buffer under an atmospheric concentration of O<sub>2</sub> (210  $\mu\text{M}$ ), (b) buffer under 1 atm of purified argon ([O<sub>2</sub>] = 0), and (c) buffer saturated with O<sub>2</sub> (1 atm of pure oxygen, [O<sub>2</sub>] = 1050  $\mu\text{M}$ ). In order to obtain various O<sub>2</sub> concentrations, different combinations of these buffers were mixed in the preparation of each experiment. Air-tight syringes were used to transfer the solutions under anaerobic conditions controlled by a dual manifold Schlenk

line. Control experiments were performed under an argon atmosphere with the same experiment techniques, where no oxidase activity was observed.

The apparent Michaelis–Menten constant of O<sub>2</sub> at 100  $\mu\text{M}$  NADPH was determined with O<sub>2</sub> concentrations ranging from 2 to 990  $\mu\text{M}$ . The binding order of NADPH and O<sub>2</sub> was studied by varying the NADPH concentration from 10 to 400  $\mu\text{M}$  over an O<sub>2</sub> concentration range of 8  $\mu\text{M}$  to 1 mM. The product inhibition by NADP<sup>+</sup> was examined with 100  $\mu\text{M}$  NADPH at both saturating (210  $\mu\text{M}$ ) and subsaturating (10  $\mu\text{M}$ ) O<sub>2</sub> concentrations. NADP<sup>+</sup> concentrations ranged from 0 to its solubility limit (~550 mM) in 200 mM Tris/HCl buffer (pH 7.9) at 37 °C. The inhibition of FDTS oxidase activity by CH<sub>2</sub>H<sub>4</sub>folate was studied by varying the CH<sub>2</sub>H<sub>4</sub>folate concentration from 0 to 100  $\mu\text{M}$  over an O<sub>2</sub> concentration range of 8  $\mu\text{M}$  to 1 mM. This inhibition study was conducted in the presence of fixed concentrations of NADPH (100  $\mu\text{M}$ ) and formaldehyde (10 mM, to stabilize CH<sub>2</sub>H<sub>4</sub>folate).

## FADH<sub>2</sub> oxidation by O<sub>2</sub>

Single-turnover experiments of the oxidative half-reaction were conducted to examine the oxidation of the enzyme bound FADH<sub>2</sub> by O<sub>2</sub>. Experiments were performed at 0 °C in 200 mM Tris/HCl buffer (pH 7.9) with a dUMP concentration range of 0–1 mM. FDTS-bound FAD (10  $\mu\text{M}$ ) was first reduced to FADH<sub>2</sub> by titrating with one equivalent of sodium dithionite [23] under anaerobic conditions. The anaerobic conditions were controlled by the Schlenk line. Reactions were then initiated by addition of O<sub>2</sub>-containing buffer ([O<sub>2</sub>] = 14  $\mu\text{M}$  in the final reaction mixture). The final volume of the reaction mixture was 300  $\mu\text{L}$ . FADH<sub>2</sub> oxidation was followed by increase of absorbance at 450 nm ( $\epsilon_{450} = 11\,300\text{ M}^{-1}\text{cm}^{-1}$ ) [12]. Data from each time course were fit to an exponential equation to obtain the rate constant for this reaction.

## Formation of the FADH<sub>2</sub>–NADP<sup>+</sup> charge-transfer complex

In order to examine the formation of the FADH<sub>2</sub>–NADP<sup>+</sup> charge-transfer complex, single-turnover experiments were conducted on the reductive half-reaction under anaerobic conditions (Ar) maintained by a glucose/glucose oxidase (type X) O<sub>2</sub>-consuming system [13]. Experiments were performed at 37 °C in 200 mM Tris/HCl buffer (pH 7.9) with 10 mM glucose, 100 units·mL<sup>-1</sup> glucose oxidase, 200  $\mu\text{M}$  NADPH and 10  $\mu\text{M}$  FDTS, at various concentrations of dUMP (0–200  $\mu\text{M}$ ). Reactions were initiated by addition of NADPH stock solution. The final volume of the reaction mixture was 300  $\mu\text{L}$ . The reduction of FAD and formation of the FADH<sub>2</sub>–NADP<sup>+</sup> complex were followed by changes in the absorbance at 450 nm [12] and in the charge-transfer band from 550 to 900 nm [17–19], respectively. Data from

each time course were fit to an exponential equation to obtain the rate constant for this process.

## Acknowledgements

This work was supported by NIH R01 GM065368 and NSF CHE- 0715448 to AK, and the Iowa Center for Biocatalysis and Bioprocessing Predoctoral Fellowships to ZW and EMK. The authors are grateful to Bryce Plapp, Daniel Quinn and Judith Klinman for insightful discussions regarding this work.

## References

- Carreras CW & Santi DV (1995) The catalytic mechanism and structure of thymidylate synthase. *Annu Rev Biochem* **64**, 721–762.
- Myllykallio H, Lipowski G, Leduc D, Filee J, Forterre P & Liebl U (2002) An alternative flavin-dependent mechanism for thymidylate synthesis. *Science* **297**, 105–107.
- Murzin AG (2002) Biochemistry: DNA building block reinvented. *Science* **297**, 61–62.
- Mathews II, Deacon AM, Canaves JM, McMullan D, Lesley SA, Agarwalla S & Kuhn P (2003) Functional analysis of substrate and cofactor complex structures of a thymidylate synthase-complementing protein. *Structure* **11**, 677–690.
- Leduc D, Graziani S, Meslet-Cladiere L, Sodolescu A, Liebl U & Myllykallio H (2004) Two distinct pathways for thymidylate (dTTP) synthesis in (hyper)thermophilic bacteria and archaea. *Biochem Soc Trans* **32**, 231–235.
- Kuhn P, Lesley SA, Mathews II, Canaves JM, Brinen LS, Dai X, Deacon AM, Elsliger MA, Eshaghi S, Floyd R *et al.* (2002) Crystal structure of thy1, a thymidylate synthase complementing protein from *Thermotoga maritima* at 2.25 Å resolution. *Protein Struct Funct Genet* **49**, 142–145.
- Agrawal N, Lesley SA, Kuhn P & Kohen A (2004) Mechanistic studies of a flavin-dependent thymidylate synthase. *Biochemistry* **43**, 10295–10301.
- Graziani S, Bernauer J, Skouloubris S, Graille M, Zhou CZ, Marchand C, Decottignies P, van Tilburg H, Myllykallio H & Liebl U (2006) Catalytic mechanism and structure of viral flavin-dependent thymidylate synthase *ThyX*. *J Biol Chem* **281**, 24048–24057.
- Griffin J, Roshick C, Iliffe-Lee E & McClarty G (2005) Catalytic mechanism of *Chlamydia trachomatis* flavin-dependent thymidylate synthase. *J Biol Chem* **280**, 5456–5467.
- Koehn EM, Fleischmann T, Conrad JA, Palfey BA, Lesley SA, Mathews II & Kohen A (2009) An unusual mechanism of thymidylate biosynthesis in organisms containing the *thyX* gene. *Nature* **458**, doi:10.1038/nature07973.
- Myllykallio H, Leduc D, Filee J & Liebl U (2003) Life without dihydrofolate reductase FoaA. *Trends Microbiol* **11**, 220–223.
- Mason A, Agrawal N, Washington MT, Lesley SA & Kohen A (2006) A lag-phase in the reduction of flavin dependent thymidylate synthase (FDTS) revealed a mechanistic missing link. *Chem Commun* **16**, 1781–1783.
- Chernyshev A, Fleischmann T, Koehn EM, Lesley SA & Kohen A (2007) The relationships between oxidase and synthase activities of flavin dependent thymidylate synthase (FDTS). *Chem Commun* **27**, 2861–2863.
- Mattevi A (2006) To be or not to be an oxidase: challenging the oxygen reactivity of flavoenzymes. *Trends Biochem Sci* **31**, 276–283.
- Segel IH (1975) *Enzyme Kinetics: Behavior and Analysis of Rapid Equilibrium and Steady State Enzyme Systems*. Wiley, New York, NY.
- Cook PF & Cleland WW (2007) *Enzyme Kinetics and Mechanism*. Taylor & Francis, New York, NY.
- Blankenhorn G (1975) Flavin-nicotinamide biscoenzymes: models for the interaction between NADH (NADPH) and flavin in flavoenzymes. Reaction rates and physicochemical properties of intermediate species. *Eur J Biochem* **50**, 351–356.
- Massey V & Ghisla S (1974) Role of charge-transfer interactions in flavoprotein catalysis. *Ann NY Acad Sci* **227**, 446–465.
- Filiseti L, Valton J, Fontecave M & Niviere V (2005) The flavin reductase ActVB from *Streptomyces coelicolor*: characterization of the electron transferase activity of the flavoprotein form. *FEBS Lett* **579**, 2817–2820.
- Hunter JH, Gujjar R, Pang CK & Rathod PK (2008) Kinetics and ligand-binding preferences of *Mycobacterium tuberculosis* thymidylate synthases, ThyA and ThyX. *PLoS ONE* **3**, e2237.
- Ulmer JE, Boum Y, Thouvenel CD, Myllykallio H & Sibley CH (2008) Functional analysis of the *Mycobacterium tuberculosis* FAD-dependent thymidylate synthase, ThyX, reveals new amino acid residues contributing to an extended ThyX motif. *J Bacteriol* **190**, 2056–2064.
- Zhou M, Diwu Z, Panchuk-Voloshina N & Haugland RP (1997) A stable nonfluorescent derivative of resorufin for the fluorometric determination of trace hydrogen peroxide: applications in detecting the activity of phagocyte NADPH oxidase and other oxidases. *Anal Biochem* **253**, 162–168.
- Gattis SG & Palfey BA (2005) Direct observation of the participation of flavin in product formation by *thyX*-encoded thymidylate synthase. *J Am Chem Soc* **127**, 832–833.

24 Motulsky H & Christopoulos A (2004) *Fitting Models to Biological Data Using Linear and Nonlinear Regression: A Practical Guide to Curve Fitting*. Oxford University Press, Oxford.

## Appendix

Here we present the details of the two analytical procedures used: (a) determination of the inhibition pattern of CH<sub>2</sub>H<sub>4</sub>folate, which is treated as a dead-end inhibitor for FDTS oxidase activity; and (b) examination and validation of the assumption that using the inhibition constant from (a) leads to direct assessment of the binding constant of CH<sub>2</sub>H<sub>4</sub>folate to the reduced and dUMP-activated enzymatic complex.

### (a) Analysis of the inhibition pattern of FDTS oxidase activity by CH<sub>2</sub>H<sub>4</sub>folate

The traditional analysis to determine the inhibition pattern [16] has been shown in the Results and Discussion. Here we present an alternative way to analyze the same data. The inhibition pattern of CH<sub>2</sub>H<sub>4</sub>folate is examined by fitting the steady-state initial velocities to the mixed-type inhibition model (Eqn A1). As presented below, this general model can distinguish between various patterns of dead-end inhibition with a single substrate and a single inhibitor:

$$\frac{v}{[E]_t} = \frac{k_{\text{cat}}[S]}{K_m \left(1 + \frac{[I]}{K_I}\right) + [S] \left(1 + \frac{[I]}{\alpha K_I}\right)} \quad (\text{A1})$$

where  $k_{\text{cat}}$  is the first-order rate constant of the reaction when [S] approaches infinity and [I] approaches zero; [S], [I] and [E]<sub>t</sub> are the concentrations of O<sub>2</sub>, CH<sub>2</sub>H<sub>4</sub>folate and total concentration of enzyme active sites, respectively;  $K_m$  is the Michaelis–Menten constant of O<sub>2</sub>; and  $K_I$  is the inhibition constant of CH<sub>2</sub>H<sub>4</sub>folate. The coefficient  $\alpha$  is the ratio between the dissociation constants of the inhibitor from the enzyme (EI) and from the enzyme–substrate complex (ESI), which reflects the difference in the inhibitor's affinities for these two different enzymatic complexes. The magnitude of  $\alpha$  discriminates between various types of inhibition [15]: when  $\alpha \ll 1$ , the inhibition is uncompetitive; when  $\alpha \sim 1$ , it is noncompetitive; and when  $\alpha \gg 1$ , it is competitive. Fitting our data to Eqn (A1) yields a value for  $\alpha$  that is much larger than unity ( $\alpha = 101 \pm 46$ ; Table A1), thus the second term of the denominator approaches [S], and the mixed inhibition model (Eqn A1) is reduced to the competitive inhibition model (Eqn 2).

**Table A1.** The kinetic parameters determined from the fittings of data for the inhibition of FDTS oxidase activity by CH<sub>2</sub>H<sub>4</sub>folate to competitive and mixed-type inhibition (Eqns 2 and A1, respectively).

Model parameter	Competitive <sup>a</sup>	Mixed-type <sup>b</sup>
$k_{\text{cat}}$ (s <sup>-1</sup> )	0.0127 ± 0.0004	0.0134 ± 0.0005
$K_m$ (μM)	7 ± 1	8 ± 1
$K_I$ (μM)	1.9 ± 0.3	2.5 ± 0.4
$\alpha$	NA	101 ± 46

<sup>a</sup> Fitted to Eqn (2) in the main text. <sup>b</sup> Fitted to Eqn (A1).

The *F*-test (a statistical test of validity of going from a complicated model to a simpler one) [24] suggests that the mixed-type inhibition (Eqn A1) does not provide a statistically better fit than the competitive inhibition (Eqn 2 in the main text). Furthermore, kinetic parameters for both fittings were determined to be identical within experimental error (Table A1). In accordance with the linearized analysis presented in the main text, the current analysis indicates that the inhibition of FDTS oxidase activity by CH<sub>2</sub>H<sub>4</sub>folate is best described by a competitive pattern.

### (b) Estimating the binding constant of CH<sub>2</sub>H<sub>4</sub>folate to the reduced and dUMP-activated enzymatic complex from its apparent inhibition constant

The analysis of data from the inhibition study of FDTS oxidase activity with CH<sub>2</sub>H<sub>4</sub>folate, presented above, treated CH<sub>2</sub>H<sub>4</sub>folate as a dead-end inhibitor. Yet, when the reduced complex is activated by dUMP [13], CH<sub>2</sub>H<sub>4</sub>folate is actually an alternative substrate competing with O<sub>2</sub>. Here we examine the validity of treating CH<sub>2</sub>H<sub>4</sub>folate as a dead-end inhibitor to assess its binding constant to the reactive enzymatic complex.

The initial velocity of the oxidase activity, in the presence of CH<sub>2</sub>H<sub>4</sub>folate, can be best described by the equation for a bi-substrate system with an alternative second substrate [15]:

$$\frac{v}{[E]_t} = \frac{k_{\text{cat}}[B]}{K_{m_B} \left(1 + \frac{K_{i_A}}{[A]} + \frac{[I]}{K_{m_I}} + \frac{K_{i_A}[I]}{K_{ii}[A]}\right) + [B] \left(1 + \frac{K_{m_A}}{[A]}\right)} \quad (\text{A2})$$

where [A], [B], [I] and [E]<sub>t</sub> are the concentrations of NADPH, O<sub>2</sub> and CH<sub>2</sub>H<sub>4</sub>folate, and total concentration of enzyme active sites, respectively;  $K_{m_A}$ ,  $K_{m_B}$  and  $K_{m_I}$  are the Michaelis–Menten constants of NADPH, O<sub>2</sub> and CH<sub>2</sub>H<sub>4</sub>folate, respectively;  $K_{i_A}$  is the dissociation constant of NADPH from the FDTS-FAD-NADPH-dUMP complex, and  $K_{ii}$  is the dissociation

